

The Increase of Radiative Lifetime of Free Excitons in Selectively Si-doped GaAs/Al_xGa_{1-x}As Heterostructures

Jurgis KUNDROTAS^{1*}, Aurimas ČERŠKUS¹, Viktorija NARGELIENĖ¹, Algirdas SUŽIEDĖLIS¹, Steponas AŠMONTAS¹, Jonas GRADAUSKAS¹, Erik JOHANNESSEN², Agnė JOHANNESSEN²

¹ Semiconductor Physics Institute of Center for Physical Sciences and Technology, A. Goštauto 11, LT-01108 Vilnius, Lithuania

² Vestfold University College, Raveien 197, 3184 Borre, Norway

crossref <http://dx.doi.org/10.5755/j01.ms.20.2.6329>

Received 29 January 2014; accepted 29 March 2014

The time resolved photoluminescence spectra of selectively Si-doped GaAs/Al_xGa_{1-x}As heterostructures have been investigated over a wide temperature range from 3.6 K to 300 K in order to identify possible mechanisms behind the observed increase in radiative lifetime of free excitons. Possible mechanisms of carrier recombination are discussed with emphasis on the unique traits of excitonic photoluminescence. The intensive lines found in the spectra of the heterostructures are associated with the formation and enhancement of free exciton emission in the flat band region of an active *i*-GaAs layer. We have established that the free exciton radiative lifetime in the heterostructures increases about two times, up to 1.44 ns in comparison with lifetime 0.6 ns of *i*-GaAs layer without a heterostructure for first sample and up to 0.92 ns from 0.4 ns for second sample at 3.6 K temperature.

Keywords: GaAs, AlGaAs, selectively doped heterostructures, photoluminescence, lifetime, exciton, time-resolved photoluminescence.

1. INTRODUCTION

Present-day research focused on high mobility devices has triggered a huge interest in the application of selectively Si-doped GaAs/Al_xGa_{1-x}As heterostructures [1, 2]. Recently GaAs/Al_xGa_{1-x}As heterostructures have been proposed as detectors of electromagnetic radiation in the microwave and terahertz ranges [3]. Although the radiative recombination processes are mainly determined by a strong internal electric field at the heterojunction interface, the origin of the photoluminescence (PL) and the nature of the recombination processes still remain unclear [4]. Bimolecular exciton formation, when an electron and a hole of an exciton are excited by different photons, is another interesting feature of the PL of GaAs/Al_xGa_{1-x}As heterostructures. This process induces superlinearities in the transient PL spectra, which can be recorded by the pump-probe experiment [5]. The dependencies of the PL intensity on temperature and excitation intensity in selectively doped GaAs/Al_xGa_{1-x}As heterostructures have demonstrated both an enhancement and narrowing of the exciton lines [6].

This paper describes the experimentally observed increase in the radiative lifetime of free excitons in selectively Si-doped GaAs/Al_xGa_{1-x}As heterostructures. A comparison to lifetime of free excitons in *i*-GaAs layers with Al_xGa_{1-x}As layer removed has been made. This action helps in part to explain the observed enhancement of the excitonic photoluminescence and the narrowing of excitonic emission line in the heterostructures.

2. SAMPLES AND EXPERIMENTAL DETAILS

Selectively Si-doped GaAs/Al_xGa_{1-x}As structures were grown by molecular beam epitaxy (MBE) on a semi-insulating GaAs substrate. Two different designs of the heterostructures, *SA* and *SD*, were investigated. The *SA* heterostructure was based on the following architecture: the AlAs mole fraction was $x = 0.25$, the thickness of the Si doped Al_xGa_{1-x}As layer was $d_{Si} = 80$ nm, the doping concentration was $N_{Si} = 10^{18}$ cm⁻³, the sheet electron concentration measured at 300 K was $n_s = 1.4 \cdot 10^{12}$ cm⁻², and the thickness of Al_xGa_{1-x}As spacer layer was $d_{sp} = 46$ nm. The architecture of the *SD* heterostructure was based on the following parameters: $x = 0.36$, $d_{Si} = 10.7$ nm, $N_{Si} = 6 \cdot 10^{18}$ cm⁻³, $n_s = 5.7 \cdot 10^{11}$ cm⁻², and $d_{sp} = 20$ nm respectively. The thickness of the active *i*-GaAs layer was 0.9 μm for both heterostructures, and a multi quantum well structure was inserted between the substrate and the active *i*-GaAs layer. More details of the *SA* and *SD* structures can be found in article [6].

The continuous wave PL was measured by a fully automated Horiba Jobin Yvon monochromator FHR-1000 with a focal length of 1000 mm. The spectra were dispersed with a blazed 1200 gr/mm grating, and the spectral dispersion was 0.8 nm/mm. The spectral resolution of the wavelength was 0.008 nm at an exit slit width of 10 μm, and the corresponding spectral resolution of the energy was 0.015 meV at 820 nm. An Ar-ion laser was used as the excitation source with an excitation energy in the range of (2.2–2.7) eV. The PL was detected by a thermoelectrically cooled Hamamatsu GaAs photomultiplier operating in the photon counting regime.

*Corresponding author. Tel.: +370-5-2619867; fax.: +370-5-2627123.
E-mail address: kundrot@pfi.lt (J. Kundrotas)

The time-resolved PL measurements were carried out using a Standa Company's frequency-doubled diode-pumped Nd:LSB microchip solid-state laser with 400 ps FWHM pulse width. The pulse repetition rate was 10 kHz, and the average output power reached 40 mW. The excitation wavelength was 531 nm (photon energy of 2.3 eV). The transient photoluminescence was measured using a Becker & Hickl time correlated single photon counting (TCSPC) system [7]. The emitted photons were detected with a thermoelectrically cooled high efficiency extended-red multi-alkali cathode photomultiplier with an internal GHz preamplifier. To avoid jitter, the measured signal was synchronized with a laser pulse from a split exciting beam. The excitation intensity was changed using neutral glass filters.

The sample temperatures were maintained from ambient room temperature (300 K) down to 3.6 K using a closed cycle helium optical cryostat (Janis Research Company 1 W @4.2 K model SHI-4). The cryostat was equipped with two thermometers; the first one used to control the operation of the equipment and the second one to measure the temperature of the sample.

3. EXPERIMENTAL RESULTS AND DISCUSSION

The PL spectra of the *SA* and *SD* heterostructures as well as that of the *i-GaAs(SA)* and *i-GaAs(SD)* active layers of the same structures at 3.6 K subject to a laser excitation intensity of 1.36 W/cm^2 , are shown in Fig. 1. The *i-GaAs* layers were prepared using chemical etching of the *SA* and *SD* heterostructures. Two distinct groups of peaks can be distinguished in the PL spectrum. The first and most intensive group is located around 1.5153 eV and is attributed to the exciton lines in the heterostructures and in the *i-GaAs* layers. The symbols X_1 and X_2 denotes the $n=1$ and $n=2$ exciton transitions, X_p indicates the exciton-polariton, $[DX]$ and $[AX]$ represents the donor and acceptor bound exciton transitions, $e-A$ is the free electron-neutral residual acceptor transition, whereas $D-A$ indicates the residual donor to residual acceptor transitions. The first emission band from the heterostructure is identified as *HB1*. This strong excitonic emission is the result of the enhancement and narrowing of the exciton line found in selectively Si-doped $\text{GaAs}/\text{Al}_x\text{Ga}_{1-x}\text{As}$ heterostructures. More details about the interpretation of the spectra and cited literature are presented in Ref. (6).

The excitonic recombination mechanism in the heterostructure is different from the recombination in the bulk *i-GaAs*. The photoexcited carriers can form excitons in the *i-GaAs* layer and may recombine back by emitting photons. However, a strong built-in electric field exists in the heterostructure. This field governs exciton formation in the close proximity of the heterointerface region. The electron-hole pairs are separated by the interface electric field. The electrons move towards the interface, whereas the holes move away from the interface. During this process the electron and hole pair remains separated, but the possibility exists that these may catch holes and electrons originating from other pairs. This formation of a

bimolecular exciton leads to the accumulation of free carriers which in turn increases the number of excitons in the flat band region of the *i-GaAs* layer. The value of the exciton line enhancement is related to the Si-doping level which causes the different electric field strength in the

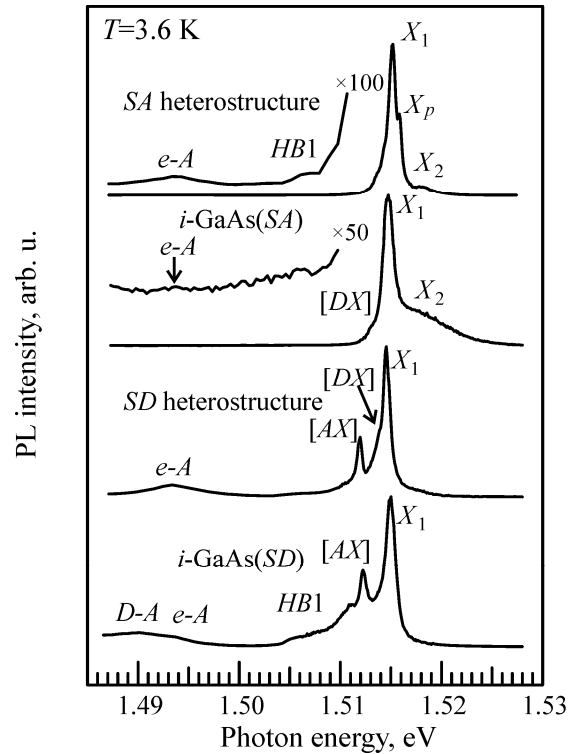


Fig. 1. The PL spectra of the *SA* and *SD* heterostructures (top curves) and the *i-GaAs(SA)* and *i-GaAs(SD)* active layers of the same structures (bottom curves). The temperature was 3.6 K and the samples were subject to a laser excitation intensity of $I = 1.36 \text{ W/cm}^2$. The symbols X_1 and X_2 indicate the $n=1$ and $n=2$ exciton transitions, X_p indicates the exciton-polariton, $[DX]$ and $[AX]$ denote the donor and acceptor bound exciton transitions, $e-A$ is the free electron-neutral residual acceptor transition, $D-A$ indicate the residual donor to residual acceptor transitions and *HB1* represents the first emission band of the heterostructure

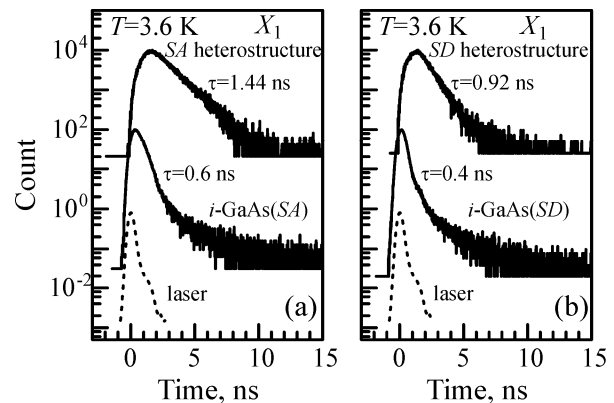


Fig. 2. The PL decay transients of free exciton X_1 emission lines of the (a) *SA* heterostructure and the *i-GaAs(SA)* and (b) *SD* heterostructure and the *i-GaAs(SD)* at an emission energy of $E = 1.5153 \text{ eV}$ and a temperature of $T = 3.6 \text{ K}$. The lowest dashed curves show the laser excitation pulse. The decay time constants are indicated at each trace. The curves are shifted vertically for clarity

i-GaAs active layer. Thus, a stronger enhancement is achieved at stronger electric fields.

The enhancement of the excitonic emission intensity is also accompanied with a narrowing of the excitonic line. The excitonic line of the heterostructure is about half as wide as that of the respective *i*-GaAs layer. Figure 2 shows the PL time evolution of the excitonic emission bands X_1 in the *SA* heterostructures and in the *i*-GaAs(*SA*) layer (Fig. 2, a), and in the *SD* heterostructures and the *i*-GaAs(*SD*) layer (Fig. 2, b) after exposing the samples to a pulsed laser excitation at a temperature of $T = 3.6$ K.

The curves were fitted by incorporating one or two exponential decay constants, and the characteristic decay times were extracted. The short lifetimes were identified after application of a deconvolution algorithm for signal processing. As a result, the decay time of the excitonic emission of the *i*-GaAs(*SA*) layer was found to be $\tau(X_1) = 0.6$ ns whereas the one for the *i*-GaAs(*SD*) layer was $\tau(X_1) = 0.4$ ns. The radiative characteristic time constant of free excitons in the heterostructures was found to be $\tau(X_1) = 1.44$ ns for the *SA* structure and $\tau(X_1) = 0.92$ ns for the *SD* structure.

The radiative lifetime of free excitons in ultrapure GaAs has been reported to be 3.3 ns at the threshold of very low (1.7 K) temperatures [8]. Since the radiative characteristic time constant of free excitons is about (0.4–0.6) ns in our *i*-GaAs layers. However, the free exciton radiative lifetimes in the heterostructures are close to the radiative lifetimes of very high quality GaAs crystals.

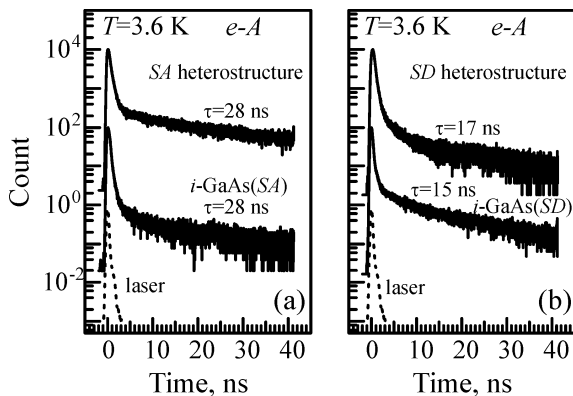


Fig. 3. The PL decay transients of free electron-residual acceptor (*e*-*A*) emission lines of (a) the *SA* heterostructures and *i*-GaAs(*SA*) and (b) the *SD* heterostructures and *i*-GaAs(*SD*) at an emission energy $E = 1.4934$ eV and a temperature of $T = 3.6$ K. The lowest dashed curves show the laser excitation pulse. The decay time constants are indicated at each trace. The curves are shifted vertically for clarity

The PL decay transients of free electron-residual acceptor (*e*-*A*) emission lines of the heterostructures and the corresponding *i*-GaAs layers at $T = 3.6$ K are presented in Figure 3. One may observe that there are no clear differences in the lifetimes from the heterostructures or the *i*-GaAs layers. This result suggests that the surface recombination mechanism is not of importance at low temperatures.

The PL decay transients of the excitonic emission lines X_1 and the band-to-band (*b*-*b*) emission bands of the heterostructures at various temperatures are presented in

Figure 4. At higher temperatures the excitonic lines merge together with the band of the *b*-*b* transitions.

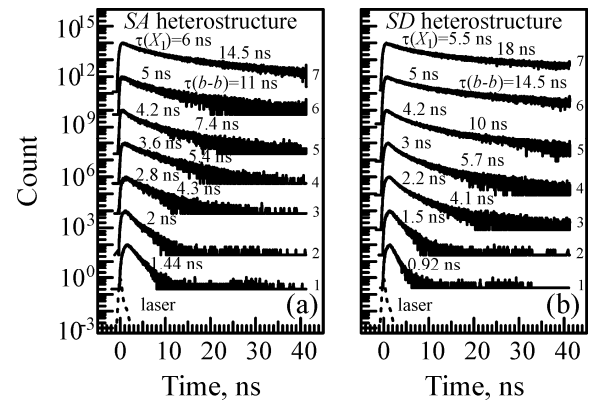


Fig. 4. The PL decay transients of emission in (a) the *SA* heterostructure and (b) *SD* heterostructure at various temperatures. The lowest dashed curves show the laser excitation pulse. $\tau(X_1)$ denotes the free exciton emission decay time constant and $\tau(b-b)$ denotes the band-to-band emission decay time constant. The constants are indicated at each trace. The curves are shifted vertically for clarity. 1 – $T = 3.6$ K, $E = 1.5153$ eV; 2 – $T = 10$ K, $E = 1.5150$ eV; 3 – $T = 20$ K, $E = 1.5144$ eV; 4 – $T = 40$ K, $E = 1.5116$ eV; 5 – $T = 77$ K, $E = 1.5042$ eV; 6 – $T = 150$ K, $E = 1.4827$ eV; 7 – $T = 300$ K, $E = 1.4247$ eV. T is the temperature, and E is the maximum emission energy, at which PL emission decay was measured

There are two characteristic times observed for both kinds of heterostructures at higher temperatures of $T \geq 20$ K. The first shorter time is attributed to the emission via excitonic states, whereas the second longer time is attributed to the band-to-band transitions.

The PL decay transients of emissions in the *SA* and *SD* heterostructures at a temperature of 40 K at various peak positions are presented in Figure 5. The insets present a continuous wave PL spectrum at 40 K. The vertical lines indicate energetic positions of the measured transients. In order to evaluate the relative weight of the different recombination processes, the PL spectra have been fitted using Elliott theory [9]. The dotted lines relate to the calculated excitonic, exciton-polaritonic and band-to-band emission contribution to the total photoluminescence intensity. The Lorentzian function broadening of the emission lines was included in the calculations. A Gaussian function was used for the polaritonic line. The broadening parameter $\Gamma = 1.2$ meV at FWHM was used for all lines [6]. The calculated results are also presented in insets of Fig. 5.

At the low energy position of the spectra (Fig. 5, position 1, curve 1), the excitonic emission dominates with the characteristic emission time constant $\tau(X_1) = 3.3$ ns for the *SA* sample and $\tau(X_1) = 3.0$ ns for the *SD* sample. At the high energy position of the spectrum (Fig. 5, position 3, curve 3) the band-to-band emission dominates with the characteristic emission time constant $\tau(b-b) = 5.4$ ns for the *SA* sample and $\tau(b-b) = 5.7$ ns for the *SD* sample. In the intermediate energy positions of the spectra (Fig. 5, position 2, curve 2) the emissions transients are more complex, because the excitonic, polaritonic and particularly the band-to-band emissions are involved.

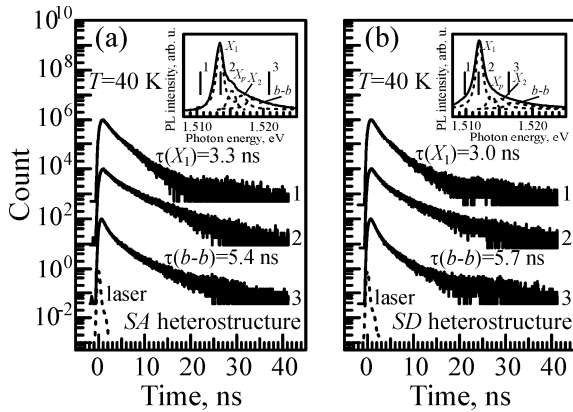


Fig. 5. The PL decay transients of the emission from the (a) *SA* and (b) *SD* heterostructure at a temperature of 40 K. The lowest curve shows the laser excitation pulse. X_1 denotes the free exciton emission decay and $b-b$ denotes the band-to-band emission decay. The decay time constants and emission energy positions are indicated at each trace. The curves are shifted vertically for clarity

The excitonic and band-to-band emissions are important at higher temperatures, and PL transients near the forbidden energy gap consist of two exponential decay curves. We conclude that the excitonic emission is important in emission processes up to room temperature. This is in agreement with previously declared experimental results obtained from continuous wave photoluminescence measurements for GaAs [10]. The estimations have shown that the excitonic emission part contributes 88 % at 22 K, 42 % at 111 K, and 14 % at 280 K of the full integrated emission intensity near the forbidden band edge.

The GaAs surfaces that are exposed to air or oxygen suffer from large density of extrinsic states that tend to fix the location of the surface Fermi level near the midgap region that result in high surface recombination velocities. The surface properties can be controlled by chemical passivation where lattice matched heterostructures are introduced, or by using a highly doped surface cap layer. At low temperatures the surface recombination does not limit the carrier lifetimes in contrast to the situation at room temperatures. The measured band-to-band recombination in GaAs heterostructures at room temperature was 2.5 μ s with a 9.8 μ m thick GaAs layer, 827 ns for a 1 μ m thick layer and 213 ns for a 0.3 μ m thick layer [11]. The thickness of the GaAs layer inserted between $\text{Al}_x\text{Ga}_{1-x}\text{As}$ layers is 0.9 μ m in our investigated samples, and the measured band-to-band radiation lifetimes at room temperature was 14.5 ns and 18 ns for the *SA* and *SD* samples, respectively. This means that the surface recombination is not important and that the recombination is controlled by the impurities, defects and phonons inside the GaAs layer. A more detailed discussion about the influence of surface on the enhancement of continuous PL intensity is presented in Ref. [12].

4. CONCLUSIONS

The time resolved photoluminescence of selectively Si-doped $\text{GaAs}/\text{Al}_x\text{Ga}_{1-x}\text{As}$ heterostructures have been investigated over a wide temperature range from 3.6 K to 300 K, with the intention to identify possible mechanisms of the increase in radiative lifetime of free excitons.

Possible mechanisms of carrier recombination are discussed with a special emphasis on the unique traits of excitonic photoluminescence. The strong intensity lines in the photoluminescence spectra of the heterostructures are associated with the formation and enhancement of free exciton emission in the flat band region of the active *i*-GaAs layer. The heterostructure was found to increase the free exciton lifetime by up to 1.44 ns in comparison to the 0.6 ns lifetime observed from a heterostructure-free *i*-GaAs sample at a temperature of 3.6 K, and up to 0.92 ns from 0.4 ns respectively for another sample. The narrowing of the excitonic line, the increase in radiative lifetime of free excitons and the existence of the exciton-polariton effect shows that the system possess a macroscopic coherence (via strong interaction of the exciton system) with the emitted electromagnetic wave in selectively doped $\text{GaAs}/\text{Al}_x\text{Ga}_{1-x}\text{As}$ heterostructures.

Acknowledgments

This work was in part supported by the Agency for Science, Innovation and Technology (grant No. 31V-37) in the frame of the High Technology Development Programme for 2011–2013.

REFERENCES

- Milnes, A. G. Semiconductor Heterojunction Topics: Introduction and Overview *Solid-State Electronics* 29 (2) 1986: pp. 99–121. [http://dx.doi.org/10.1016/0038-1101\(86\)90029-8](http://dx.doi.org/10.1016/0038-1101(86)90029-8)
- Kiehl, R. A., Gerhard Sollner, T. C. L. (Eds.). High Speed Heterostructure Devices. Semiconductors and Semimetals. 41. Boston, San Diego: Academic Press, 1994.
- Suziedėlis, A., Ašmontas, S., Požela, J., Kundrotas, J., Širmulis, E., Gradauskas, J., Kozič, A., Kazlauskaitė, V., Anbinderis, T. Mesoscopic Structures for Microwave-THz Detection *Acta Physica Polonica A* 113 (3) 2008: pp. 803–809.
- Shen, J. X., Pittini, R., Oka, Y. Strong anti-Stokes Photoluminescence of GaAs Free Excitons in $\text{GaAs}/\text{Ga}_{1-x}\text{Al}_x\text{As}$ Heterojunctions *Physical Review B* 64 (19) 2001: p. 195321. <http://dx.doi.org/10.1103/PhysRevB.64.195321>
- Shen, J. X., Pittini, R., Oka, Y. Superlinear Photoluminescence Intensity Observed in Pump-Probe Experiments in $\text{GaAs}/\text{Ga}_{1-x}\text{Al}_x\text{As}$ Heterojunctions *Physica Status Solidi (b)* 221 (1) 2000: pp. 545–548.
- Kundrotas, J., Čerškus, A., Nargelienė, V., Suziedėlis, A., Ašmontas, S., Gradauskas, J., Johannessen, A., Johannessen, E., Umansky, V. Enhanced Exciton Photoluminescence in the Selectively Si-doped $\text{GaAs}/\text{Al}_x\text{Ga}_{1-x}\text{As}$ Heterostructures *Journal of Applied Physics* 108 (6) 2010: p. 063522 (7).
- Becker, W. The bh TCSPC Handbook: Fourth Edition. Berlin: Becker & Hickl GmbH, 2010.
- Hoof, G. W., van der Poel, W. A. J. A., Molenkamp, L. W., Foxon, C. T. Giant Oscillator Strength of Free Excitons in GaAs *Physical Review B* 35 (15) 1987: pp. 8281–8284. <http://dx.doi.org/10.1103/PhysRevB.35.8281>
- Elliott, R. J. Theory of Excitons-I. In: Polarons and Excitons. Eds. Kuper, C. G., Whitfield, G. D., Edinburgh: Oliver & Boyd Ltd, 1963: pp. 269–293.
- Grilli, E., Guzzi, M., Zamboni, R., Pavesi, L. High-precision Determination of the Temperature Dependence of the Fundamental Energy Gap in Gallium Arsenide *Physical Review B* 45 (4) 1992: pp. 1638–1644
- Gilliland, G. D., Wolford, D. J., Kuech, T. F., Bradley, J. A., Hjalmanson, H. P., Minority-carrier Recombination Kinetics and Transport in "Surface-free" $\text{GaAs}/\text{Al}_x\text{Ga}_{1-x}\text{As}$ Double Heterostructures *Journal of Applied Physics* 73 (12) 1993: pp. 8386–8396. <http://dx.doi.org/10.1063/1.353407>
- Čerškus, A., Nargelienė, V., Kundrotas, J., Suziedėlis, A., Ašmontas, S., Gradauskas, J., Johannessen, A., Johannessen, E. Enhancement of the Excitonic Photoluminescence in n^+i -GaAs by controlling the Thickness and Impurity Concentration of the n^+ Layer *Acta Physica Polonica A* 119 (2) 2011: pp. 154–157.